The interannual variability of southerly low-level jets in North America

Lejiang Yu[a,b,c], Shiyuan Zhong[b,c*], Julie A. Winkler[b], Dana L. Doubler[b], Xindi Bian[d], and Claudia K. Walters[e]

[a] Polar Research Institute of China, Shanghai, China
[b] Department of Geography, Michigan State University, East Lansing, Michigan
[c] Center for Global Change and Earth Observations, Michigan State University, East Lansing, Michigan

[d] U.S. Forest Service, Northern Research Station, Lansing, Michigan
[e] Department of Social Sciences, University of Michigan-Dearborn, Dearborn, Michigan

*Corresponding Author: Shiyuan Zhong, Ph.D.
Department of Geography
Michigan State University
673 Auditorium Rd., East Lansing, MI 48823
Phone: (517)-432-4743, Fax: (517) 432-1617, Email: zhongs@msu.edu

ABSTRACT: The interannual variability of southerly low-level jets (SLLJs) over North America during the warm (April-September) and cool (October-March) seasons is investigated. SLLJ occurrences over a 31-year period (1979-2009) were identified from the North American Regional Reanalysis (NARR) vertical wind profiles. The first empirical orthogonal function (EOF) modes of the SLLJ frequency during the warm and cool seasons account for about 30% and 20% of the total variance, respectively. Both modes can be interpreted as a strengthening or weakening of the core area of SLLJ anomalies. The principal component (PC) time series display significant positive trends, suggesting an increase in SLLJ activity during both seasons on interdecadal time scales and are significantly correlated to the summertime Pacific Decadal Oscillation (PDO) and Atlantic Multidecadal Oscillation (AMO) for the warm season and the wintertime PDO, AMO and El Niño Modoki for the cool season. The second modes account for about 20% and 15% of the total variance for the warm and cool seasons, respectively, and are interpreted as primarily a subseasonal latitudinal shift in SLLJ activity between the central Great Plains and the western Gulf of Mexico and southern Texas during the warm season and a longitudinal shift between the western Gulf of Mexico and the Caribbean during the cool season. The second mode appears to be significantly correlated to El Niño Modoki for the warm season and to Niño 3.4 for the cool season.

KEY WORDS Southerly low-level jet; Empirical orthogonal functions (EOF); the Pacific Decadal Oscillation (PDO); El Niño Southern Oscillation (ENSO); El Niño Modoki

1. Introduction

A low-level jet (LLJ) is an atmospheric phenomenon characterized by strong horizontal wind speeds in the lower troposphere. LLJs can occur from all directions, but in North America, they are usually characterized by strong low-level winds from either northerly (referred to as northerly LLJ or NLLJ) or southerly (referred to as southerly LLJ or SLLJ) directions. SLLJs are particularly significant for North America as they transport warm humid air into the continental interior. SLLJs are often linked to severe weather conditions including thunderstorms, heavy precipitation, and tornadic activity (Augustine and Caracena, 1994; Zhong et al., 1996; Arritt et al., 1997; Wu and Raman, 1998; Walters and Winkler, 2001; Winkler, 2004; Svoma, 2010; Weaver et al., 2012). While SLLJs have been observed across all of North America, they occur most often in the Great Plains east of the Rocky Mountains (Bonner, 1968; Walters et al., 2008), over the western Gulf of Mexico (Doubler et al., 2015), along the Mid-Atlantic coast (Zhang et al., 2006), and over the Gulf of California and southwestern Arizona (Douglas, 1995; Anderson et al., 2001; Ralph et al., 2005; Doubler et al., 2015). In all four areas, more than 50% of the SLLJs occur at night (Doubler et al., 2015), although jets have been observed any time of day.

SLLJs are more frequent in the Great Plains of the United States than any other regions in North America, and, not surprisingly, the Great Plains SLLJs are the most studied. Numerous previous studies have investigated the mechanisms responsible for SLLJ formation and, in general, have found that a single mechanism alone is unable to explain the occurrence and characteristics of observed jets (Stensrud, 1996; Zhong et al., 1996; Igau and Nielsen-Gammon, 1998). Blackadar (1957) argued that an inertial oscillation near the friction layer can help induce a SLLJ, and later Wu and Raman (1998) attributed inertial oscillations as the main mechanism for nocturnal SLLJ formation in the Great Plains. The elevated topography of the Rocky Mountains, and the resulting differential heating, also is an important reason for the formation of Great Plains SLLJs (Wexler, 1961; Holton, 1967). Besides boundary-layer forcing, synoptic processes can induce and strengthen SLLJs. For example, SLLJs may be attributed to coupling with an upper tropospheric jet streak within its exit region (Uccellini and Johnson, 1979; Sjostedt et al., 1990; Wu and Raman, 1998). Also, changes in the pressure gradient force associated with leeside troughing and cyclogenesis can influence the development of SLLJs in the Great Plains (Uccellini, 1980).

The mechanisms responsible for SLLJs over the western Gulf of Mexico are less well understood. Several authors have suggested that SLLJs in this area may represent a northward-turning branch of the easterly Caribbean jets (Amador, 2008; Cook and Vizy, 2010), whereas others suggest that SLLJs form through interactions with an onshore sea breeze, inertial oscillation and nocturnal stabilization of the boundary layer (Nielsen-Gammon, 2006; Tucker et al., 2010). Synoptic forcing such as a developing upper-level trough can also force northward airflow over the Gulf of Mexico (Igau and Nielsen-Gammon, 1998), especially during the cool season. Gulf of California SLLJs are also not as well studied, although they are thought to often form in response to nighttime cooling and the consequent horizontal temperature gradients over the sloped orography of the foothills of the Sierra Madre (Anderson et al., 2001). Synoptically forced "surged events" with strong southeasterly airflow can also contribute to the formation of Gulf of California SLLJs (Anderson et al., 2001). SLLJs over the Mid-Atlantic states have been linked to thermal gradients associated with the Appalachian Mountains and with the Chesapeake Bay and the Atlantic Ocean (Zhang et al., 2006).

Most previous SLLJ studies focused on boundary-layer or synoptic processes with a temporal scale of a few hours to a week. But several studies examined the relationship between large-scale circulation and sea-surface temperature (SST) anomalies and the occurrence and characteristics of SLLJs at interannual and decadal time scales (Song et al., 2005; Ting and Wang, 2006; Weaver et al., 2009; 2012). Based on numerical simulations, Ting and Wang (2006) suggested that variations in the strength of the Bermuda High and the associated trade winds over the Caribbean Sea and the Gulf of Mexico contribute to interannual variations in Great Plains SLLJ strength. Song et al. (2005) noted that fewer (more) SLLJs occurred in the southern Great Plains during the major El Niño (La Niña) episodes and the warm (cool) phase of the Pacific Decadal Oscillation (PDO) in the period of 1997-2002. In a recent study, Krishnamurthy et al. (2015) found that stronger Great Plains SLLJs appear to be related to La Niña in boreal spring (April-June), while the relationship is opposite in boreal summer (July-September). In contrast, Harding and Snyder (2015) reported that strong Great Plains SLLJ events predominantly occur with negative values of the Pacific-North American teleconnection pattern. Another recent study by Liang et al. (2015) found that the Central Pacific El Niño during its decaying phase can weaken the Great Plains SLLJs. Using Empirical Orthogonal Function (EOF) analysis to investigate the variability of summertime Great Plains SLLJs during 1958-2001, Weaver and Nigam (2008) noted that the first three EOFs were linked to post-peak-phase El Niño-Southern Oscillation (ENSO), pre-peak-phase ENSO, and the summer North Atlantic Oscillation (NAO), respectively. They also found, in a second study (Weaver et al., 2009), that the connection between the Great Plains SLLJs and SST variability in the warm season appears to be strongest during the July-September period. They later (Weaver et al. 2012) associated the springtime (April-June) North American SLLJs with the Atlantic Multidecadal Oscillation (AMO) SST structure for the period of 1950 to 1978, but with the PDO SST structure for the period of 1979 to 2010.

In the current study, we further investigate the low-frequency variability of North American SLLJs and expand on earlier analyses in a number of important ways. Similar to several earlier analyses (Weaver and Nigam, 2008; Weaver et al., 2009, 2012), EOF analysis is used to identify dominant spatial patterns of SLLJ variability. However, we apply the EOF analysis to frequencies of SLLJs identified directly from 3-hourly vertical wind profiles. Our jet definitions are similar to those employed in classical jet climatologies (e.g., Bonner, 1968) that include criteria for maximum wind speed and vertical wind shear both above and below the maximum, in contrast to defining SLLJs in terms of monthly or seasonal meridional wind anomalies on fixed (e.g., 925 hPa) pressure levels as employed in most earlier studies of low-frequency variability (Weaver and Nigam, 2008; Weaver et al., 2009; 2012). One motivation for the use of jet frequencies rather than wind speed anomalies is the contrasting interpretation of jet frequency for the western Gulf of Mexico, where analyses based on low-level meridional wind anomalies suggest frequent summertime SLLJs (e.g., Cook and Vizy, 2010) and those that included a vertical shear criterion indicating infrequent SLLJs at this time of year (Rife et al., 2010; Doubler et al., 2015). Also, the lack of a fixed elevation in our jet definition acknowledges that SLLJs can occur at a range of elevations within the lower troposphere, and that some jets, particularly those that are primarily synoptically forced, may have slantwise airflow. Another contribution is a larger domain over which the spatial variability is analyzed that captures other areas of high SLLJ frequency in addition to the Great Plains region. The analysis also separately considers the spatial modes of variability for warm (April-September) and cool (October-March) season SLLJs, given that the relative contribution of different jet mechanisms likely varies seasonally. In addition, the analysis presented below explicitly investigates the interannual variability of the different spatial modes of SLLJ frequency, and the association of these time series with the interannual variations of large-scale circulation variables and indices.

The rest of the paper is organized as follows: Section 2 describes the data and methods used in the study. Section 3 begins with a general description of the jet climatology, which is followed by a discussion of the leading modes of the interannual variability and the possible connection to large-scale circulation anomalies. Section 4 compares the results from the current analysis with those of previous studies and discusses the implications and limitations of this study. The paper concludes in Section 5.

2. Data and methods

SLLJs were defined from the vertical wind profiles of the North American Regional Reanalysis (NARR, Mesinger et al., 2006). NARR is produced by the National Centers for Environmental Prediction (NCEP) using the operational NCEP regional Eta model and its data assimilation system (Mesinger et al., 1988; Janjic, 1994). NARR has a horizontal resolution of 32 km, and the data are archived starting from 1979 at 29 vertical levels (13 levels in the lower troposphere below 700 hPa) with a 3-hourly temporal resolution.

SLLJs were extracted for all NARR grid points between 10°N-60°N and 140°W-50°W, which covers the continental United States, southern Canada, Mexico, and the Intra-Americas (Figure 1). In this study a SLLJ was identified if a wind profile satisfies all of the following four criteria: 1) wind direction from 113˚-247˚, 2) a wind speed maximum e 12 m s^{-1} at or below 3000 m above ground level (AGL), 3) a decreasing wind speed by e 6 ms^{-1}above the maximum wind level to the next minimum or to 5000 m AGL (whichever was lower), and 4) a decreasing wind speed by e 6 ms^{-1} below the maximum wind level. The same jet definition was previously employed by Doubler et al. (2015) to identify SLLJs from NARR wind profiles. This definition differs from that previously used by Bonner (1968) in his classic climatological analysis of Great Plains LLJs in two ways. First, Bonner's criterion only considered the maximum speed and the decreasing rate above the level of the maximum speed but the current definition considers the addition of a shear criterion below the maximum speed level as used by several previous authors (Andreas et al., 2000; Banta et al., 2002; Walters and Winkler, 2001; Walters et al., 2008). Second, this definition include jets that occur up to 3000 m AGL in the lower troposphere in contrast to a 1500 m AGL ceiling used by Bonner, allowing for the inclusion of synoptic-forced jets in addition to boundary-layer forced jets. Our criteria for SLLJs are similar to those used in Walters et al. (2014) in their comparison of NARR-derived and rawinsonde-observed SLLJs over the Great Plains with the exception that they used 700 hPa and 500 hPa instead of 3000 m and 5000 m AGL. The criteria were applied to the 3-hourly wind profiles at every NARR grid point in the study domain for the period of 1979 to 2009. The use of NARR instead of other available sources of upper-level wind profiles is supported by the comparisons of Walters et al. (2014) who found that, although NARR tended to underestimate SLLJ frequency compared to rawinsonde observations, the spatial patterns and diurnal variations of relative jet frequency are similar between the two datasets and that the NARR frequencies appear to be less sensitive to discontinuities introduced by changes in instrumentation and observing practices compared to the rawinsonde-derived jet frequencies.

EOF analysis was utilized to identify the dominant spatial and temporal patterns of the interannual variability for North American SLLJ frequency. EOF analysis produces a set of modes that consist of spatial structures (EOFs) and corresponding time series (principal components [PCs]). For each mode, its EOF and PC are orthogonal to the EOFs and PCs of all other modes. Each mode has a corresponding eigenvalue that describes the variance explained by that mode. The EOF analysis was performed separately for the warm (April-September) and cool (October-March) seasons, and applied to SLLJ frequency anomalies with respect to the 1979-2009 seasonal climatologies over the entire domain shown in Figure 1. The two-season grouping follows the convention used by Whiteman et al. (1998) in their climatological analysis of the Great Plains LLJs and by Zhang et al. (2006) in their study of the jets in the Mid-Atlantic states. Both studies focused on jets in the warm season defined as May through September. Here, we extend the warm season to include April because April is a month with high SLLJ frequency (Doubler et al., 2015), and because it allows an even division of the year into two seasons. The EOF results that will be presented below are from unrotated EOF analysis. The results of rotated EOFs are similar but show less variance explained by the first two modes than those of unrotated EOFs.

To explore possible relationships between the temporal changes in the dominant modes of SLLJ frequency anomalies and the changes in the atmospheric circulation patterns, the PC time series were correlated with time series of six well-known teleconnections: 1) the Niño3.4 index defined as Pacific SST anomalies in the region bounded by 90°W-150°W and 5°S- 5°N (Trenberth, 1997) (available at http://www.cpc.ncep.noaa.gov/data/indices/), 2) the El Niño Modoki index that captures anomalous warming in the central tropical Pacific and cooling in the eastern and western tropical Pacific (Askok et al., 2007) (available at http://www.jamstec.go.jp/frsgc/research/d1/iod/modoki_home.html.en), 3) the Pacific Decadal Oscillation (PDO) index defined as the leading principal component of North Pacific monthly SST variability (Mantua et al., 1997) (available at http://jisao.washington.edu/pdo/PDO.latest), 4) the Pacific North American (PNA) index that summarizes differences in 500 hPa geopotential height between the northern Pacific Ocean and the North American continent (Barnston and Livezey, 1987) (available at http://www.cpc.ncep.noaa.gov/products/precip/CWlink/pna/pna_index.html), 5) the North Atlantic Oscillation (NAO) index representing differences in sea-level pressure between the Icelandic low and the Azores high (Barnston and Livezey, 1987) (available at http://www.cpc.ncep.noaa.gov/products/precip/CWlink/pna/nao_index.html) and 6) the Atlantic Multidecadal Oscillation (AMO) index that is derived from the SST over the North Atlantic Ocean (0 to 70°N) and represents a mode of natural variability occurring in the North Atlantic Ocean on multidecadal time scales (Enfield et al., 2001) (available at http://www.esrl.noaa.gov/psd/data/timeseries/AMO/).

To help further understand the association between large-scale circulation and SLLJ variability, linear regression was performed following the approach of Weaver and Nigam (2008) where the fields of 200 hPa and 925 hPa geopotential height, 925 hPa winds, and SST anomalies were regressed to the PC time series. Global gridded fields of 200 hPa geopotential height were obtained from the NCEP-Department of Energy (DOE) global reanalysis-2 dataset (Kanamitsu et al., 2002) which has a horizontal resolution of T62 (~209km); SST anomalies were extracted from the Extended Reconstructed SST version 3 (ERSSTv3) dataset (Smith et al., 2008), which has a 2° latitude x 2° longitude resolution; and 925 hPa geopotential heights and winds were extracted from the aforementioned NARR dataset with a 32 km resolution. Regression analyses were performed at each grid point of the respective datasets, and the regression coefficients provide a measure of the direction and magnitude of the association of the climate anomaly parameters at a specific grid point with the leading EOF patterns of SLLJ variability and can be interpreted as the variations at each grid point in the atmospheric variables with changes in the PC.

3. Results and discussion

3.1 Annual and seasonal mean jet frequency

Before we explore the leading modes of the variability in SLLJ occurrences, we first examine the 31-year climatology of the annual mean and warm- and cool-season mean SLLJ frequencies over North America. The annual mean and the warm- and cool-season means exhibit a similar spatial pattern with elevated frequencies found in a relatively narrow band about 1000 km wide in the central U.S., stretching from the northern plains to the western Gulf of Mexico (Figure 2). This pattern is consistent with what was found by earlier SLLJ climatological studies (Bonner, 1968; Mitchell et al., 1995; Walters et al., 2008). Within this band, jet frequencies exceed 10% in three distinct centers -- the border between Kansas and

Oklahoma, western/central Texas, and southern Texas/western Gulf of Mexico. In addition to these centers of elevated jet frequencies, jet frequencies > 5% extend southward over the Yucatan Peninsula and northward into the northern plains and western Great Lakes region. Frequencies fall below 5% for the Gulf of California jets and the Mid-Atlantic state jets.

While the jet frequency over the southernmost center at the southern Texas/western Gulf of Mexico border shows little seasonal dependency, at the other two centers, jets are more frequent (15-20%) during the warm season compared to the cool season (10-15%). In addition, the position of the middle center moves slightly eastward from western/central Texas in the warm season to central Texas in the cool season. Jets over the Yucatan Peninsula and the Gulf of California are less frequent during the cool season than the warm season, whereas they are more frequent in Mid Atlantic states in the cool season. Areas of elevated jet frequencies > 10 % also appear along Canada's west coast and the eastern boundary of the Gulf of Alaska in the cool season, due possibly to the frequent wintertime cyclogenesis in the Gulf of Alaska (Businger and Walter, 1988).

3.2 Interannual Varibility

3.2.1 *Warm season*

EOF analysis is performed for the SLLJ warm-season anomalies during the 31-year study period and the percentages of the total variance explained by the first ten EOF modes are shown in Table 1. Because the first two modes together explain nearly 50% of the total variance, the analyses shown below will focus only on the first two modes. The first mode, which explains 30% of the total variance and represents the most frequently realized spatial pattern, is dominated by increases in warm-season SLLJ frequencies over central United States and western North Atlantic and a decrease in southern Canada. There are large SLLJ anomalies of up to 5% in the Great Plains, particularly over the southern plains and the western Gulf of Mexico, with smaller anomalies of the same sign observed over the western Atlantic (Figure 3a). Variations of smaller magnitude (< 2%) but opposite sign (i.e., negative frequency anomalies) are evident in northern Canada over Hudson Bay. The time series of the first mode, i.e., PC1, displays marked interdecadal variability (Figure 3c). Prior to 1999, PC1 is negative, which corresponds to negative SLLJ frequency anomalies over the southern plains/western Gulf of Mexico/western Atlantic and positive anomalies over Hudson Bay; the pattern reversed after 1999. The positive temporal trend in the PC1 time series suggests that the frequency of SLLJs in the southern plains/western Gulf of Mexico/western Atlantic has increased since 1987.

The second EOF mode, accounting for about 20% of the total variance and representing the second most frequent spatial pattern, is dominated by a dipole between the western Gulf of Mexico and the central plains (Figure 3b), suggesting that when SLLJs are frequent in the central plains they are infrequent over the western Gulf of Mexico and vice versa. A weaker dipole pattern is also seen between the Caribbean Sea and the northwestern Atlantic Ocean. The time series of the second mode (PC2) (Figure3d) shows substantial interannual variation, but little temporal trend. The difference between the maximum (+2.4) in 2002 and the minimum (-2.6) in 1998 is striking, which according to the EOF2 spatial pattern (Figure 3b), corresponds to a significant increase in the Great Plains jets and a significant decrease in the Gulf of Mexico jets in 2002, and the opposite in 1998.

Correlation analysis of the PC1 time series with the time series of the various teleconnections (Table 2) for each month in the warm season suggests a strong positive relationship with the AMO index (correlation coefficients ranging from 0.36 to 0.52, all statistically significant at the 95% confidence level) and negative association with the PDO index (correlation coefficients -0.38 in April and -0.41 in July). For PC2, a strong positive association is found with the El Nino Modoki index (correlation coefficients ranging from 0.39 in May to 0.58 in August, all significant at the 95% confidence level), although PC2 also is correlated significantly with PNA in September (correlation coefficient -0.41) and NAO in April (correlation coefficient 0.45). In short, the interdecadal variability and trend of PC1are related to the warm-season PDO and AMO indices; the interannual variability of PC2 is associated with El Nino Modoki.

To further understand the spatial patterns of the leading two EOF modes in the context of atmospheric circulation anomalies, the time series of the first two EOF modes were regressed to the anomalies of warm-season SST, 200 hPa geopotential height (H200), and 925 hPa geopotential height (H925) and winds. The regression coefficients are shown in Figures 4 and 5 for the first and second EOF modes, respectively. The coefficients for H200 suggest that positive PC1 values (i.e., anomalously high frequencies of SLLJs in the southern plains/western Gulf of Mexico) are associated with a wave train at mid and high latitudes with positive H200 anomalies centered over northeastern Asia and the northern Pacific at approximately 60°N and 160°E, negative anomalies north of approximately 40°N over North America, and negative anomalies north of 70°N over the northeastern Atlantic and Greenland (Figure 4a), whereas the opposite pattern (upper-level ridging over northern North America and troughing over northeastern Asia/north Pacific) is associated with negative PC1 values (i.e., decreased frequency of SLLJs in the southern plains/western Gulf of Mexico). The spatial pattern of the coefficients for the regressions between PC1 and SST resembles a negative-phase PDO in North Pacific Ocean (Mantua et al., 1997), characterized by warm SST anomalies in the central north Pacific (largest anomalies are located at approximately 40°N and 170°E) and cool anomalies in northeastern Pacific (centered around 15°N and 140°W), and a positive-phase AMO with warm SST anomalies over the North Atlantic Ocean (north of 45°N) (Figure 4b). This interpretation is in agreement with the positive correlation of PC1 with AMO and negative correlation with PDO discussed above (Table2).

At 925 hPa, negative geopotential height anomalies occur over the U.S., southern Canada, and the tropical eastern Pacific Ocean (Figure 4c). Corresponding to these anomalous height patterns are the occurrences of southerly wind anomalies over the Gulf of Mexico and the south central Great Plains of the United States and the western North Atlantic Ocean, contributing to increased SLLJ activities in these regions.

The spatial patterns of the regression coefficients for the second EOF mode (Figure 5) differ considerably from those of the first mode. Positive coefficients, reflective of positive H200 anomalies, are again found over northeastern Asia and negative coefficients prevail across northern North America (Figure 5a), although this pattern is confined to higher latitudes (north of approximately 55°N) compared to the first mode. Negative coefficients are found over the central Pacific Ocean, and positive values over central North America; both anomalies are focused around 40°N. Thus, the second EOF mode, with anomalously high values of SLLJ frequency over the south-central plains and reduced frequency over the western Gulf of Mexico, is associated with ridging over the United States. As anticipated given the strong correlations between PC2 and the El Niño Modoki index, the spatial pattern of the regression coefficients for SST is reflective of an El Niño Modoki pattern (Ashok et al. 2007) with negative values over the tropical Pacific Ocean east of the 120° W and west of the 150°E and positive values between the two longitudes (Figure 5b). Positive regression coefficients for H925 over the eastern U.S. and Canada indicate that frequent SLLJs in the central plains occur with a strong, westward extending Bermuda High that drives the location of the frequency maximum northwards (Figure 5c and 5d). Anomalous northerly winds over the Gulf of Mexico would suppress SLLJ occurrences in this region.

3.2.2 *Cool season*

The first mode for the cool season, which accounts for 24% of the total variance compared to 30% for the warm season (Table 1), is focused on the south central United States and western

Gulf of Mexico (Figure 6a). The time series of the first mode (PC1) shows a significant increasing trend (Figure 6c), indicating that the frequency of SLLJs in the south central U.S. and the western Gulf of Mexico during the cool season has increased since approximately 1993.

The second mode accounts for 15% of the total variance compared to 20% for the warm season, and exhibits variations that are of opposite sign between the eastern Gulf of Mexico (and to a lesser extent northeastern Canada) and the rest of the domain, but particularly with the Caribbean Sea off the Yucatan Peninsula (Figure 6b). Thus, when fewer than average SLLJs occur over the western Gulf of Mexico, SLLJs are more frequent than average over the Caribbean and vice versa. The time series of the second mode (PC2) displays little temporal trend but strong interannual variability (Figure 6d).

Significant correlations with the time series of PC1 are found for several of the teleconnection indices (Table2). Correlations with the NAO are particularly large for January and March when the correlation coefficients are -0.43 and -0.46, respectively, significant at the 95% confidence level. Significant negative correlations between PC1 and the PDO index are found in October (-0.37), February (-0.44), and March (-0.53), whereas the most significant correlations with the El Niño Modoki index occur in January (-0.39), February (-0.46), and March (-0.37). PC1 is correlated significantly with the Niño 3.4 index in February and March with coefficients of -0.36 and -0.42, respectively. In contrast, strong positive correlations are observed between PC1 and AMO for all months in the cool season, with large correlation coefficients of 0.56-0.67 for October through January. For PC2, the strongest correlation is found with Niño3.4 with correlation coefficients of 0.6-0.7 across the months during the cool season. PC2 is also significantly correlated with PNA in January through March. In addition PC2 has a significant positive correlation with PDO and AMO in February and March and a negative correlation with NAO in February. In sum, the interdecadal variability and trend of the cool-season PC1is related to the AMO, PDO and El Niño Modoki. But, unlike the warm season, the interannual variability of the cool-season PC2 is influenced by ENSO.

The PC time series of the first two EOF modes were regressed with the time series of the cool-season anomalies of SST, H200, H925, and 925 hPa winds, with the results shown in Figure 7. The regression maps for PC1 show similar patterns to those found for the warm season, which is not a surprise given the significant correlations with PDO and AMO for both seasons. The H200 coefficients display a distinct wave pattern (Figure 7a), suggesting that positive values of PC1 are associated with positive H200 anomalies over the north central Pacific Ocean (centered around 40°N and 170°W), the southwestern U.S. (at approximately 35°N and 110°W) and northeastern North America, Greenland, and the western North Atlantic Ocean north of 55°N, and with negative H200 anomalies over the tropical North Pacific Ocean near 20°N and 170°W, northwestern North America around 55°N and 140°W, the northeastern Atlantic Ocean near 40°N and 10°W, and eastern Asia north of 40°N. The spatial pattern of the regression coefficients for SST (Figure 7b) suggests a negative phase of PDO over the mid and high latitudes of the Pacific Ocean (north of 20°N), an El Niño Modoki pattern over the tropical

Pacific Ocean (20°N-20°S), and a positive phase of AMO over the northern Atlantic Ocean (north of 0°), in agreement with the correlations between PC1 and these circulation indices. The H925 height and wind anomalies (Figure 7c and 7d) indicate that the anticyclone in the western Atlantic centered around 30°N and 60°W produces anomalous southerly and southwesterly airflow over the Gulf of Mexico and the southern and central U.S., leading to increased occurrences of SLLJs (Figure 7c and 7d).

The most notable feature of the regression maps of PC2 with H200 are the large negative values, reflective of troughing, over the central and northern Pacific north of approximately 35°N and large positive values, reflective of riding over the tropical Pacific south of 20°N (Figure 8a). These centers extend eastward with troughing over the western and central United States, and ridging over the Intra-Americas. Large positive coefficients representing upper-level ridging are also found over northeastern Canada between 50-60°N. In accordance with the large positive correlations between PC2 and the Nino 3.4 index, the spatial pattern of the SST regression coefficients resembles an El Niño pattern (Trenberth, 1997) with negative SST anomalies over the tropical central western Pacific Ocean (120°E-160E, 20°N-20°S) and positive SST anomalies over the tropical central eastern Pacific Ocean (160°E-80°W, 15°N-20°S) (Figure 8b).

Positive H925 height anomalies occur over northeastern North America north of approximately 50°N, while negative values occur over the rest of the study domain (Figure 8c). A weak cyclonic cell seen in the H925 anomaly wind fields over the southeastern U.S. at approximately 30°N and 85°W is associated with anomalous northerly airflow over the southern plains and western Gulf of Mexico and an expected decrease in SLLJ frequency, and with anomalous southwesterly airflow over the Caribbean Sea and the tropical western Atlantic Ocean and an expected increase in SLLJ occurrences (Figure 8d). The anomalous southeasterly winds over the central U.S. and western Canada play a similar role in the anomalous occurrences of SLLJs.

4. Summary and Discussion

In this study, EOF analyses were performed to investigate the interannual variability of the frequency of SLLJ occurrences over North America during warm (April-September) and cool (October-March) seasons. The SLLJ frequencies were determined using 3-hourly vertical wind profiles in the NARR dataset from 1979-2009 and a jet definition that, similar to those employed in previous jet climatologies (e.g., Walters and Winkler, 2001; Walters, 2008; Walters et al., 2014; Doubler et al., 2015), includes criteria for both maximum wind speed and vertical wind shear. The leading modes of spatial variability were identified for each season and the connections to variations in large-scale circulation patterns were explored via correlation and regression analyses. The results not only substantiate those from previous studies but also provide new insights into SLLJ variability over a larger North American domain that captures other areas of relatively high SLLJ frequency, most notably the western Gulf of Mexico, in addition to the Great Plains region of the United States.

The first two EOF modes for the warm-season SLLJ frequency resemble the spatial variability modes identified earlier by Weaver and Nigam (2008) from NARR wind fields, even though in their study the EOF analysis was performed on May-June 900-hPa meridional wind anomalies (as a surrogate for SLLJ frequency) rather than directly on jet frequencies. This similarity points to the robustness of the spatial variability patterns.

Weaver and Nigam (2008) interpreted their first mode, which was dominated by positive anomalies over the southern plains, as a strengthening/expansion of the Great Plains SLLJ core. A strengthening, although not necessarily an expansion, of the region with greatest SLLJ anomalies is also an appropriate interpretation for the leading EOF of SLLJ frequencies presented here, given that the largest anomalies associated with EOF1 overlie the area of greatest warm season jet frequency. An important distinction, though, is that the largest anomalies are found over the southern plains, outside of what some consider the "core" region of the warm season Great Plains SLLJ. Thus, we would describe the first mode more broadly as a strengthening (weakening) of SLLJ frequencies over a broad area including the southern plains, western Gulf of Mexico and the western Atlantic, when the corresponding PC1 values are positive (negative). Another important difference is that the PC1 time series presented in Weaver and Nigam (2008) does not display a strong temporal trend, in contrast to the significant positive trend found for the PC1 time series obtained when EOF analysis is directly applied to SLLJ frequencies. Thus, the interpretation that the frequency of SLLJs in the southern plains/western Gulf of Mexico/western Atlantic has increased with time is unique to this study.

Weaver and Nigam's (2008) second mode of variability, with positive anomalies over the central plains and negative anomalies over the western Gulf of Mexico, also has similarities with the EOF2 pattern presented here. They interpreted this EOF as a northward-shift in the Great Plains SLLJ. A modified interpretation is that EOF2 reflects latitudinal shifts in the location of centers of maximum jet frequency. As seen in Figure 2, multiple centers of enhanced jet frequency are found in the Great Plains and the western Gulf of Mexico during the warm season, and Doubler et al. (2015) found that the timing of the greatest activity for these centers differed, with the largest SLLJ frequencies in the southern plains and western Gulf of Mexico occurring April-May, and the largest frequencies in the central plains occurring later in the warm season from approximately June-September. Thus, we interpret EOF2 as representing subseasonal latitudinal shifts in the locations of maximum SLLJ frequency. The PC2 time series for both studies display considerable interannual variability, but little temporal trend.

An intriguing observation is the substantial differences in the spatial-temporal modes of SLLJ variability identified by Weaver et al. (2012) for springtime SLLJs over the U.S., Mexico, and Gulf of Mexico and the variability modes identified in this study and Weaver and Nigam (2008). Weaver et al.'s (2012) EOF1 is focused farther north over the central plains, even when allowing for the southward shifts in location that they observed from 1950 to 2010, in contrast to the southern plains for the other two studies. In addition, Weaver et al.'s second mode suggests a longitudinal dipole between the northern plains and the eastern U.S., rather than latitudinal shifts between the central and southern plains. These differences arise even though this study and Weaver et al. (2012) analyzed SLLJ activity over a considerably larger spatial domain than Weaver and Nigam (2008). However, Weaver et al. (2012) employed a coarser dataset (the 2.5° resolution NCAR-NCEP reanalysis), in contrast to the 32 km resolution NARR dataset employed in the other two studies, and focused on SLLJs at a higher (850 hPa) elevation.

The regression analyses presented here for warm season SLLJs provide some insights on the synoptic-scale forcing contributing to jet occurrence. In particular, the regressions of the time series of PC1with H925 grid point anomalies suggest that SLLJs in the southern plains are associated with leeside cyclogenesis, as inferred from the negative regression coefficients (i.e., negative height anomalies) to the east of the southern Rocky Mountains when the value of PC1 is positive. The negative coefficients for the PC1 and H200 regressions also point to the presence of upper-level troughing over central North America. By extension, SLLJs would be less frequent in the southern plains when anomalously high 925 hPa heights are located over the south central United States and northern Mexico and when upper-level ridging is present over central North America. In contrast, the regressions of PC2 with H925 suggest that frequent warm season SLLJ activity over the central plains (i.e., positive PC2) occurs with positive H925 height anomalies (i.e., an anticyclone) centered over the eastern United States and extending into the northern Gulf of Mexico and an upper-level ridge over the central

United States. The contrasting synoptic patterns inferred from the H925 regression analyses imply that grouping SLLJs under the general umbrella of "Great Plains" SLLJs masks differences in jet characteristics and forcing, including temporal trends in jet frequency. The inferred H925 synoptic patterns also differ from the findings of Weaver et al. (2009) who argued that a low-level anticyclone (positive sea-level pressure anomaly) is centered over the Gulf of Mexico during greater Great Plains SLLJ activity, particularly in July-September.

The regression analyses also point to some uncertainty in the sign of SST anomalies during enhanced warm season SLLJ activity. Whereas Weaver et al. (2009) found stronger SLLJs in the Great Plains occurred with a warm Pacific and a cool Atlantic, our findings suggest that only SLLJs frequency anomalies in the central plains (EOF2) are associated with a warm Pacific, and that SLLJs anomalies in the southern plains/western Gulf of Mexico (EOF1) occur with a cool eastern Pacific. In contrast, little association with SSTs over the western Atlantic or the Gulf of Mexico is observed for either EOF.

The EOF analysis of cool season SLLJ frequencies is a new contribution to the literature on low-frequency SLLJ variability. The leading EOF mode for the cool season can be interpreted as a strengthening or weakening of the jet core, similar to the interpretation of EOF1 for warm season SLLJs, although the largest frequency anomalies extend southeastward into the western Gulf of Mexico compared to the warm season when the largest anomalies are centered on eastern Texas. EOF2, on the other hand, appears to represent a longitudinal shift in jet frequencies, with positive frequency anomalies over the Caribbean Sea and negative anomalies over the western Gulf of Mexico (or vice versa). The regression analyses with the PC2 time series suggest that upper-level troughing over the southwestern U.S. and a cyclone over the northern Gulf of Mexico and southeastern U.S. contribute to reduced SLLJ activity in the western Gulf of Mexico and enhanced activity over the Caribbean Sea. Concomitantly, above average jet frequencies over the western Gulf of Mexico are associated with upper-level ridging over the southwestern and south central United States and a broad anticyclone over the southern United States and Gulf of Mexico. The significant positive trend seen for PC1 suggests that SLLJ frequency is increasing in the cool season as well as in the warm season.

The larger study domain of our analysis provided some interesting insights on the co-variations of SLLJ frequency across North America and the Intra-Americas. In particular, warm season SLLJs are less (more) frequent over Hudson Bay when jet frequencies across the southern plains are higher (lower). On the other hand, Gulf of California jets , although frequently mentioned in the literature, were not reflected in the first two variability modes of warm season SLLJs, suggesting that a larger number of EOFs are needed to extract information on these jets. Another area where SLLJs are frequent but does not appear clearly in the first two EOFs is the Mid-Atlantic states, although a very weak frequency anomaly immediately off the Mid-Atlantic coast is seen for EOF2 during the warm season.

The correlations of the PC time series for each EOF suggest linkages between SLLJ frequency and large-scale circulation, and several of the findings agree with those of previous analyses. For instance, the negative correlation between annual variations in the frequency of warm season SLLJs and the PDO index has been uncovered by previous researchers (Song et al., 2005; Weaver et al., 2012). Also, Weaver et al. (2012) previously noted a possible association between North American SLLJ occurrences and a SST pattern resembling El Niño Modoki. In addition, the dipole structure of the warm season EOF2 shown here is similar to the spatial pattern of SLLJ speed associated with El Nino Modoki shown in Liang et al. (2015), although the extent of their positive anomalies in the dipole is smaller and located farther north. Additional insights that have not previously been described in the literature include the apparent relationships of cool season variations in jet frequency with AMO, PDO, and ENSO. Furthermore, the positive trends in warm season and cool season SLLJ frequency appear to be related to trends in AMO and PDO, given the strong correlations between these teleconnection indices and PC1 for both seasons.

5. Conclusions

Based on the EOF and regression analyses presented, we can draw the following conclusions about the spatial patterns and time changes of the interannual variability of the SLLJ frequencies over North American and their relationships to known climate anomalies for the warm season and for the cool season:

- The first EOF modes, which account for about 30% and 20% of the total variance for the warm season and cool season, respectively, can both be interpreted as a general increase in the SLLJ frequencies over the central United States with further strengthening of jet core region in the southern Great Plains and western Gulf of

Mexico at interdecadal time scale.

- Positive trends exhibited by the PC1 time series for both the warm and the cool season suggest increased SLLJ activities over time in the abovementioned regions.
- The second modes account for about 20% and 15% of the total variance for the warm and cool seasons, respectively, and can be interpreted as primarily a subseasonal latitudinal shift in SLLJ activity between the central plains and the Gulf of Mexico and southern Texas during the warm season, and a longitudinal shift between the western Gulf of Mexico and the Caribbean during the cool season.
- The time variations of the first modes appear to be significantly correlated to the summertime Pacific Decadal Oscillation (PDO) and Atlantic Multidecadal Oscillation (AMO) for the warm season and the wintertime PDO, AMO and El Niño Modoki for the cool season. The time changes for the second modes are significantly correlated to El Niño Modoki for the warm season and to Niño 3.4 for the cool season.

Understanding the variability and predictability of SLLJs, a conduit for massive transport of warm and moist air from the Gulf of Mexico into central US, is crucial to the prediction of convective precipitation over the United States. The relationships between SLLJ frequency anomalies and the SST anomalies over the Pacific and Atlantic Oceans established from the analysis here can be used to improve seasonal predictions of heavy precipitation in the U.S. for both the warm and cool seasons. These relationships could also be useful for seasonal forecasts of wind resources in the U.S. and the surrounding oceans.

Although analyses of SLLJ spatial and temporal variability have numerous practical applications, the comparisons presented above between the findings of this study and earlier investigations of SLLJ variability point to the potential impact of the conditions of the EOF, correlation, and regression analyses on the interpretation of SLLJ variability. While the inclusion of a vertical shear criterion in the SLLJ definition appears to have only a small influence on the EOF and other outcomes, the elevation at which the low-level wind anomalies are defined may have a larger impact on the statistical outcomes. In addition, the spatial resolution of the dataset used to identify SLLJ occurrences appears to influence the statistical depiction of spatial and temporal SLLJ variability. Additional research is needed to evaluate the influence of the choice of time period and the definition of seasons and subseasons on the EOF-identified variability modes, the correlations with atmospheric teleconnections, and the geopotential height, low-level winds, and sea-surface temperature anomalies. These additional analyses are essential to better incorporate SLLJ variability into seasonal forecasts of regional precipitation and wind resources. It is also worth noting that the results presented here are only statistical explanations for the two leading interanuual variability modes of SLLJs during the warm and cool seasons. Further analyses, including numerical simulations of how SSTs over the north Pacific and Atlantic Oceans influence SLLJs over the central U.S. and the Gulf of Mexico, are needed to better understand the mechanisms contributing to the spatial and temporal variability of North American SLLJs and to further improve seasonal SLLJ predictions.

Acknowledgements

The research was supported partially by the National Science Foundation under Grants BCS-0924768 and BCS-0924816 and by AgBioResearch of Michigan State University. The authors would like to thank NCEP for the NARR dataset.

References

Anderson BT, Roads JO, Chen SC, Juang HMH. 2001. Model dynamics of summertime low-level jets over northwestern Mexico. *J. Geophys. Res.: Atmos.* **106**: 3401-3413.

Andreas EL, Claffey KJ, Makshtas AP. 2000. Low-level atmospheric jets and inversions over the western Weddell Sea. *Bound.-Layer Meteor*. **97**: 459-486.

Ashok K, Behera SK, Rao SA, Wen H, Yamagata T. 2007. El Niño Modoki and its possible teleconnection. *J. Geophys. Res.* **112**: C11007. DOI: 10.1029/2006JC003798.

Arritt RW, Rink TD, Segal M, Todey DP, Clark CA, Mitchell M.J, Labas KM. 1997. The Great Plains low-level jet during the warm season of 1993. *Mon. Wea. Rev.* **125**(9): 2176-2192.

Augustine JA, Caracena FC. 1994. Lower-tropospheric precursors to nocturnal MCS development over the central United States. *Wea. Forecasting* **9**(1): 116-135.

Barandiaran D, Wang S-Y, Hilbum K. 2013 Observed trends in the Great Plains low-level jet and associated precipitation changes in relation to recent droughts. *Geophys. Res. Lett.* **40**: L058296.

Barnston AG, Livezey RE. 1987. Classification, seasonality and persistence of low-frequency atmospheric circulation patterns. *Mon. Wea. Rev.* 115:1083-1126.

Banta RM, Newsom RK, Lundquist JK, Pichugina YL, Coulter RL, Mahrt L. 2002. Nocturnal low-level jet characteristics over Kansas during CASES-99. *Bound.-Layer Meteor.* **105**: 221-252.

Blackadar AK. 1957. Boundary layer wind maxima and their significance for the growth of nocturnal inversions. *Bull. Amer. Meteor. Soc.* **38**: 282-290.

Bonner WD. 1968. Climatology of the low-level jet. *Mon. Wea. Rev.* **96**: 833-850.

Businger S, Walter B. 1988. Comma cloud development and associated rapid cyclogenesis over the Gulf of Alaska: A case study using aircraft and operational data. *Mon. Wea. Rev.* **116**: 1103-1123.

Doubler DL, Winkler JA, Bian X, Walters CK, Zhong S. 2015. A NARR-derived climatology of southerly and northerly low-level jets over North America and coastal environs. *J. Appl. Meteor. Climatol.* **54**: 1596-1619.

Douglas MW. 1995. The summertime low-level jet over the Gulf of California. *Mon. Wea. Rev.* **123**: 2334-2347.

Enfield DB, Mestas-Nunez AM, Trimble PJ. 2001. The Atlantic Multidecadal Oscillation and its relationship to rainfall and river flows in the continental U.S. *Geophys. Res. Lett*. **28**: 2077-2080.

Harding KJ, Snyder PK. 2015. The Relationship between the Pacific–North American Teleconnection Pattern, the Great Plains Low-Level Jet, and North Central U.S. Heavy Rainfall Events. *J. Climate* **28**: 6729-6742.

Holton JR. 1967. The diurnal boundary layer wind oscillation above sloping terrain. *Tellus* **19**: 199-205.

Igau RC, Nielson-Gammon JW. 1998. Low-level jet development during a numerically simulated return flow event. *Mon. Wea. Rev.* **126**: 2972-2990.

Janjic ZI. 1994. The step-mountain Eta coordinate model: further developments of the convection, viscous sublayer, and turbulence closure schemes. *Mon. Wea. Rev.* **122**: 927-945.

Kanamitsu M, Ebisuzaki W, Woollen J, Yang S-K, Hnilo JJ, Fiorino M, Potter GL. 2002: NCEP/DOE AMIP-II Reanalysis (R-2). *Bull. Amer. Meteor. Soc.* **83**: 1631–1643.

Kao H-Y, Yu J-Y. 2009: Constrasting seatern-Pacific and central-Pacific types of ENSO. *J. Climate* **22**: 615-632.

Krishnamurthy L, Vecchi GA, Msadek R, Wrrtenberg A, Delworth TL, Zeng F. 2015: The seasonality of the Great Plains low-level jet and ENSO relationship. *J. Climate* **28**: 4525-4544.

Liang Y-C, Yu J-Y, Lo M-H, Wang C. 2015. The changing influence of El Niño on the Great Plains low-level jet. *Atmos. Sci. Let.* DOI: 10.1002/assl.590.

Mantua NJ, Hare SR, Zhang Y, Wallace JM, Francis RC. 1997. A Pacific interdecadal climate oscillation with impacts on salmon production. *Bull. Amer. Meteor. Soc.* **78**: 1069-1079.

Mesinger F, Janjic ZI, Nickovic S, Gavrilov D, Deaven DG. 1988. The step-mountain coordinate-model description and performance for cases of Alpine lee cyclogenesis and for a case of an Appalachian redevelopment. *Mon. Wea. Rev.* **116**: 1493-1518.

Mesinger F, DiMego G, Kalnay E, Mitchell K, Shafran PC, Ebisuzaki W, Jovi D, Woollen J. Rogers E, Berbery EH, Ek MB, Fan Y, Grumbine R, Higgins W, Li H, Lin Y, Manikin

G, Parrish D, Shi W. 2006. North American regional reanalysis. *Bull. Amer. Meteor. Soc.* **87**: 343-360.

Ralph FM, Neiman PJ, Rotunno R. 2005. Dropsonde observations in low-level jets over the northeastern Pacific Ocean from CALJET-1998 and PACJET-2001: Mean vertical-profile and atmospheric-river characteristics. *Mon. Wea. Rev.* **133**: 889-910.

Rife DL, Pinto JO, Monaghan AJ, Davis CA, Hannan JR. 2010. Global distribution and characteristics of diurnally varying low-level jets. *J. Climate* **23**: 5041-5064.

Smith TM, Reynolds RW, Peterson TC, Lawrimore J. 2008. Improvements to NOAA's historical merged land-ocean surface temperature analysis (1880-2006). *J. Climate* **21**: 2283-2296.

Sjostedt DW, Sigmon JT, Colucci SJ. 1990. The Carolina nocturnal low-level jet: synoptic climatology and a case study. *Wea. Forecasting* **5**: 404-415.

Song J, Liao K, Coulter RL, Lesht BM. 2005. Climatology of the low-level jet at the southern Great Plains atmospheric boundary layer experiments site. *J. Appl. Meteor.* **44**: 1593-1606.

Stensrud DJ. 1996. Importance of low-level jets to climate: a review. *J. Climate* **9**: 1698-1711.

Svoma BM. The influence of monsoonal gulf surges on precipitation ad diurnal precipitation patterns in central Arizona. *Wea. Forecasting* **25**: 281-289.

Ting M, Wang H. 2006. The role of the North America topography on the maintenance of the Great Plains summer low-level jet. *J. Atmos. Sci.* **63**: 1056-1068.

Trenberth KE. 1997. The definition of El Niño. *Bull. Amer. Meteor. Soc.* **78**: 2771-2777.

Uccellini LW, Johnson DR. 1979. Coupling of upper and lower tropospheric jet streaks and implications for the development of severe convective storms. *Mon. Wea. Rev.* **107**: 682-703.

Uccellini LW. 1980. On the role of upper tropospheric jet streaks and leeside cyclogenesis in the development of low-level jet in the Great Plains. *Mon. Wea. Rev.* **10**8: 1689-1696.

Walters CK, Winkler JA. 2001. Airflow configurations of warm season southerly low-level wind maxima in the Great Plains: Part I. Spatial and temporal characteristics and relationship to convection. *Wea. Forecasting* **16**(5): 513-530.

Walters CK, Winkler JA, Shadbolt RP, van Ravensway J, Bierly GD. 2008. A long-term climatology of southerly and northerly low-level jets for the central United States. *Ann. Assoc. Amer. Geogr.* **98**: 521-552.

Walters CK, Winkler JA, Husseini S, Keeling R, Nikolic J, Zhong S. 2014. Low-level jets in the North American Regional Reanalysis (NARR): A comparison with rawinsonde observations. *J. Appl. Meteorl. Clim.* **53**: 2093-2113.

Weaver SJ, Nigam S. 2008. Variability of the Great Plains low-level jet: Large-scale circulation context and hydroclimate impacts. *J. Climate* **21**: 1532-1551.

Weaver SJ, Schubert S, Wang H. 2009. Warm season variations in low-level circulation and precipitation over the central United States in observations, AMIP simulations, and idealized SST experiments. *J. Climate* **22**: 5401-5420.

Weaver SJ, Baxter S, Kumar A. 2012. Climatic role of North American low-level jets on U.S. regional tornado activity. *J. Climate* **25**: 6666-6683.

Wexler H. 1961. A boundary layer interpretation of the low-level jet. *Tellus* **13**: 368-378.

Winkler JA. 2004. The impact of technology upon in situ atmospheric observations and climate science. *Geography and Technology,* Kluwer Academic Publishers: Dordrecht, The Netherlands.

Wu Y, Raman S. 1998. The summertime Great Plains low level jet and the effect of its origin on moisture transport. *Bound.-Layer Meteor.* **88**(3): 445-466.

Zhang D-L, Zhang S, Weaver SJ. 2006. Low-level jets over the Mid-Atlantic States: warm-season climatology and a case study. *J. Appl. Meteorl. Clim.* **45**: 194-209.

Zhong S, Fast JD, Bian X. 1996. A case study of the Great Plains low-level jet using wind profiler network data and a high-resolution mesoscale model. *Mon. Wea. Rev.* **124**: 785-806.

Table 1. The percentage of the total variance explained by the first ten EOF modes.

Modes	1st	2nd	3rd	4th	5th	6th	7th	8th	9th	10th
Warm season	30.40	19.75	12.76	4.97	3.05	2.85	2.60	2.37	2.17	1.94
Cool season	23.78	15.40	9.94	6.98	6.21	4.56	3.92	3.27	2.42	2.23

Table 2. Correlation coefficients between the Principal Components (PC) for the first two EOF modes of SLLJ variability and teleconnections for each month of the warm and cool seasons. *Indicates significant above 95% confidence level using student's t-test.

	Warm Season						**Cool Season**					
Index	APR	MAY	JUN	JUL	AUG	SEP	OCT	NOV	DEC	JAN	FEB	MAR
				EOF1								
Niño 3.4	-0.23	-0.17	-0.07	-0.03	-0.04	-0.04	-0.14	-0.19	-0.27	-0.32	-0.36*	-0.42*
El Niño Modoki	-0.19	-0.11	-0.06	-0.09	-0.08	0.00	-0.25	-0.22	-0.29	-0.39*	-0.46*	-0.37*
PDO	-0.38*	-0.35	-0.22	-0.41*	-0.34	-0.34	-0.37*	-0.32	-0.20	-0.28	-0.45*	-0.53*
PNA	-0.23	-0.25	-0.15	0.19	0.09	0.00	-0.06	0.04	-0.07	-0.43*	-0.27	-0.46*
NAO	-0.14	-0.29	-0.13	-0.27	-0.22	0.16	-0.12	-0.22	-0.25	0.05	-0.05	0.01
AMO	0.42*	0.38*	0.36*	0.40*	0.51*	0.52*	0.64*	0.64*	0.67*	0.56*	0.48*	0.30
				EOF 2								
Niño 3.4	0.00	0.10	0.20	0.27	0.28	0.28	0.70	0.70*	0.69*	0.67*	0.64*	0.60*
El Niño Modoki	0.32	0.39*	0.53*	0.54*	0.58*	0.57*	0.31	0.27	0.10	0.16	0.17	0.11
PDO	-0.09	-0.08	-0.03	-0.02	0.09	0.04	0.21	0.15	0.25	0.34	0.47*	0.48*
PNA	-0.12	-0.05	0.35	0.14	0.00	-0.41*	-0.04	0.00	0.35	0.37 *	0.49*	0.37*
NAO	0.45*	0.16	0.19	0.12	-0.22	-0.03	-0.25	0.18	0.09	0.13	-0.50*	-0.18
AMO	0.05	-0.12	-0.18	-0.14	-0.09	-0.01	0.11	0.11	0.06	0.28	0.45*	0.58*

Figure captions

Figure 1. Study domain (10°-70° N, 140°-50° W) with topography (m above MSL).

Figure 2: Mean SLLJ frequency (expressed as a percentage of NARR time steps) (a) annually, (b) during the warm season (April-September), and (c) during the cool season (October-March) for the period 1979-2009.

Figure 3. Spatial patterns (panels a and b) and time series of the corresponding principal components (panels c and d) of the two leading EOF modes of SLLJ frequency during the warm season for 1979-2009.

Figure 4. The anomalous (a) 200 hPa geopotential height (gpm), (b) sea surface temperature (°C), (c) 925 hPa geopotential height (gpm) and (d) wind field (m/s) maps regressed to the time series of the first EOF mode of warm season SLLJ frequency for the period 1979-2009. The filled regions are significant at the 95% confidence level.

Figure 5. The anomalous (a) 200 hPa geopotential height (gpm), (b) sea surface temperature (°C), (c) 925 hPa geopotential height (gpm) and (d) wind field (m/s) maps regressed to the time series of the second EOF mode of warm season SLLJ frequency for the period 1979-2009. The filled regions are significant at the 95% confidence level.

Figure 6. Same as Figure 3, but for the cool season.

Figure 7. Same as Figure 4, but for the cool season.

Figure 8. Same as Figure 5, but for the cool season.

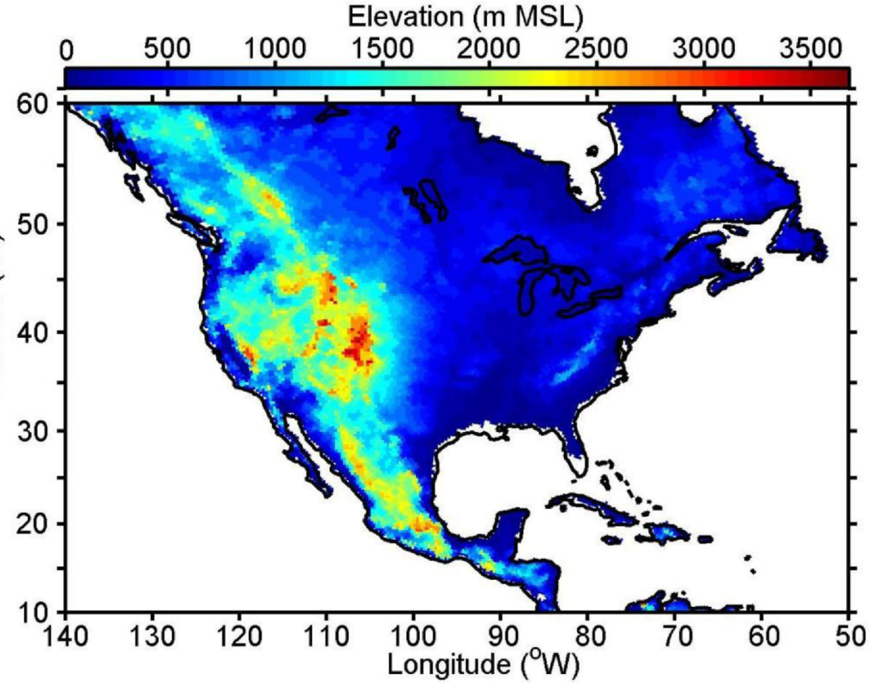
Elevation (m MSL)
0
500
1000
1500
2000
2500
3000
3500
60
50
40
30
20
10
Latitude (°N)
140
130
120
110
100
90
80
70
60
50
Longitude (°W)

figure1

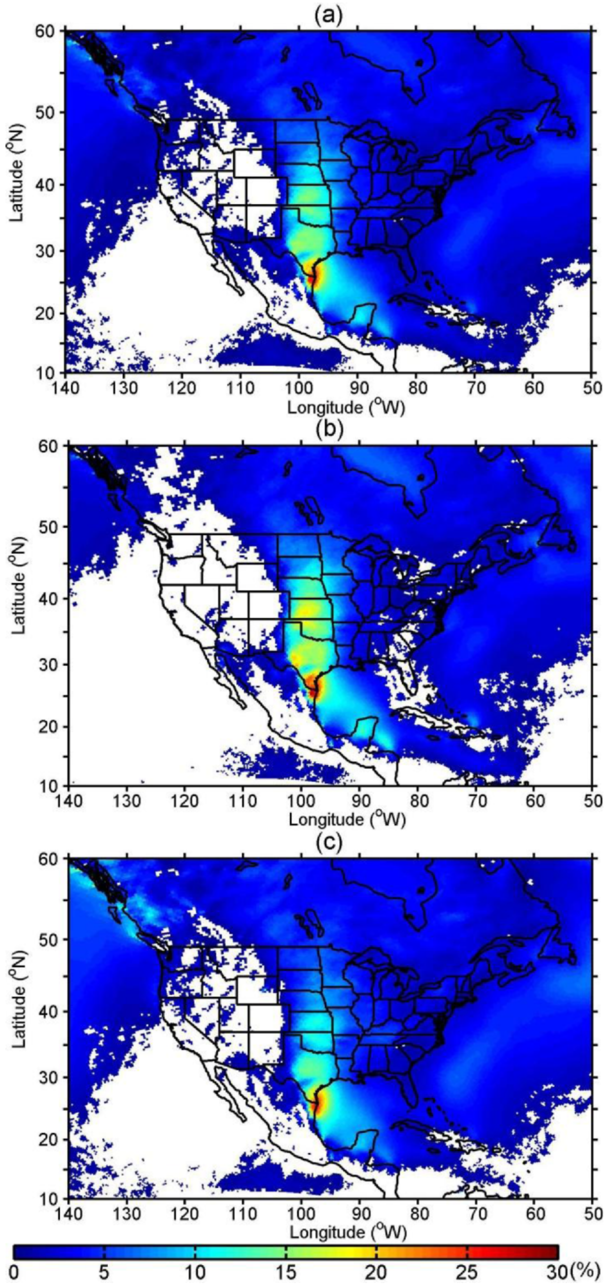
(a)
(b)
(c)
Latitude (°N)
60
50
40
30
20
10
Longitude (°W)
140
130
120
110
100
90
80
70
60
50
0
5
10
15
20
25
30(%)

figure2

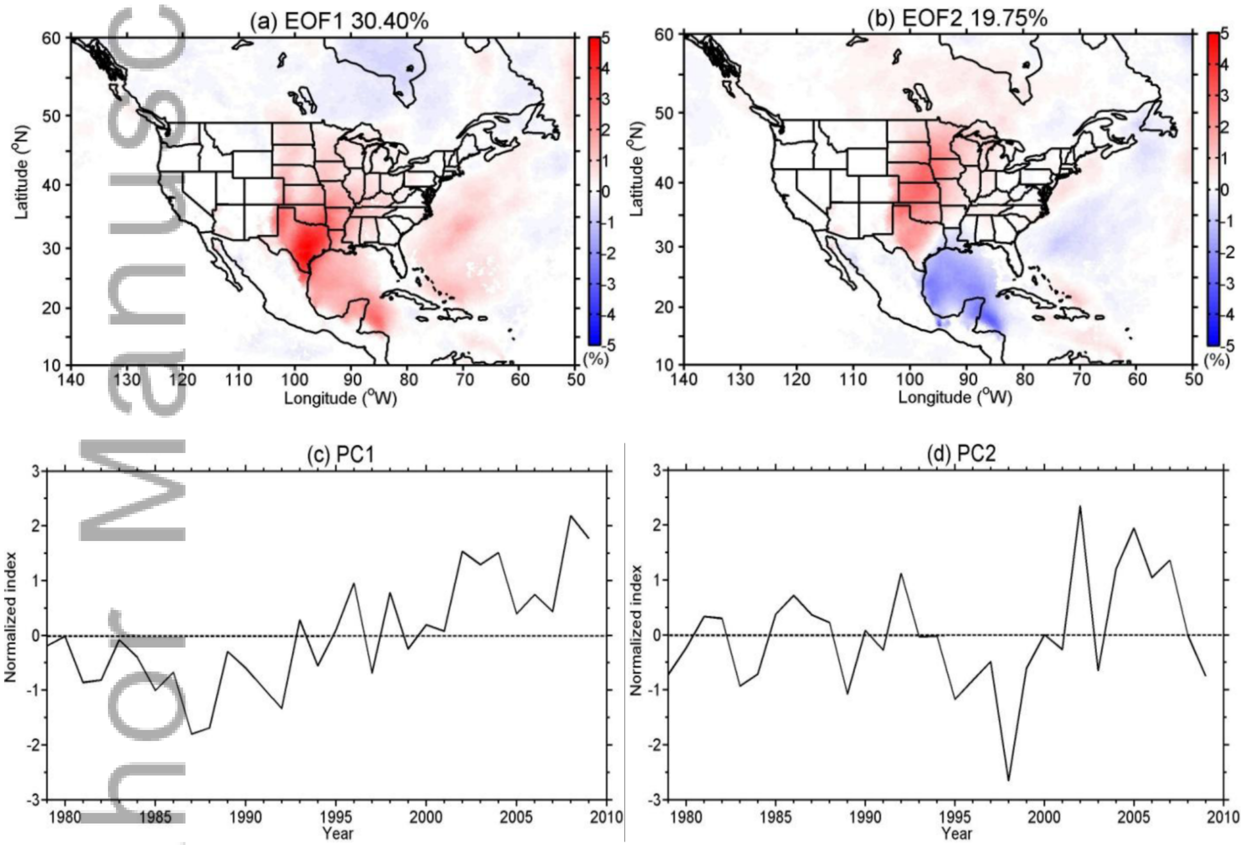
(a) EOF1 30.40%
(b) EOF2 19.75%
Latitude (°N)
Longitude (°W)
(%)
(c) PC1
(d) PC2
Normalized index
Year

Figure3.tif

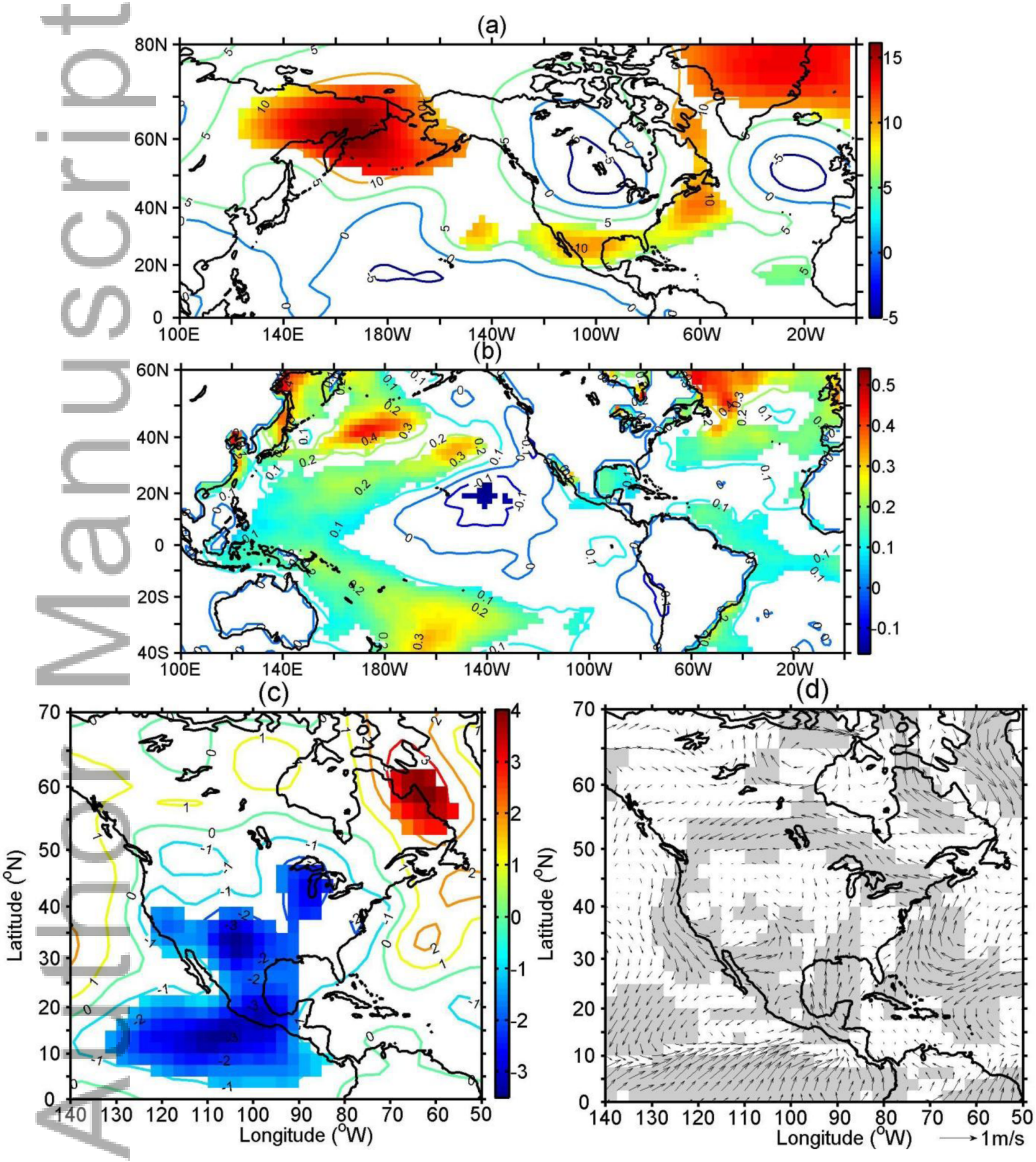
(a)
80N
60N
40N
20N
0
100E
140E
180W
140W
100W
60W
20W
15
10
5
0
-5
(b)
60N
40N
20N
0
20S
40S
0.5
0.4
0.3
0.2
0.1
0
-0.1
(c)
Latitude (°N)
Longitude (°W)
140 130 120 110 100 90 80 70 60 50
70 60 50 40 30 20 10 0
4
3
2
1
0
-1
-2
-3
(d)
1m/s

Figure4.tif

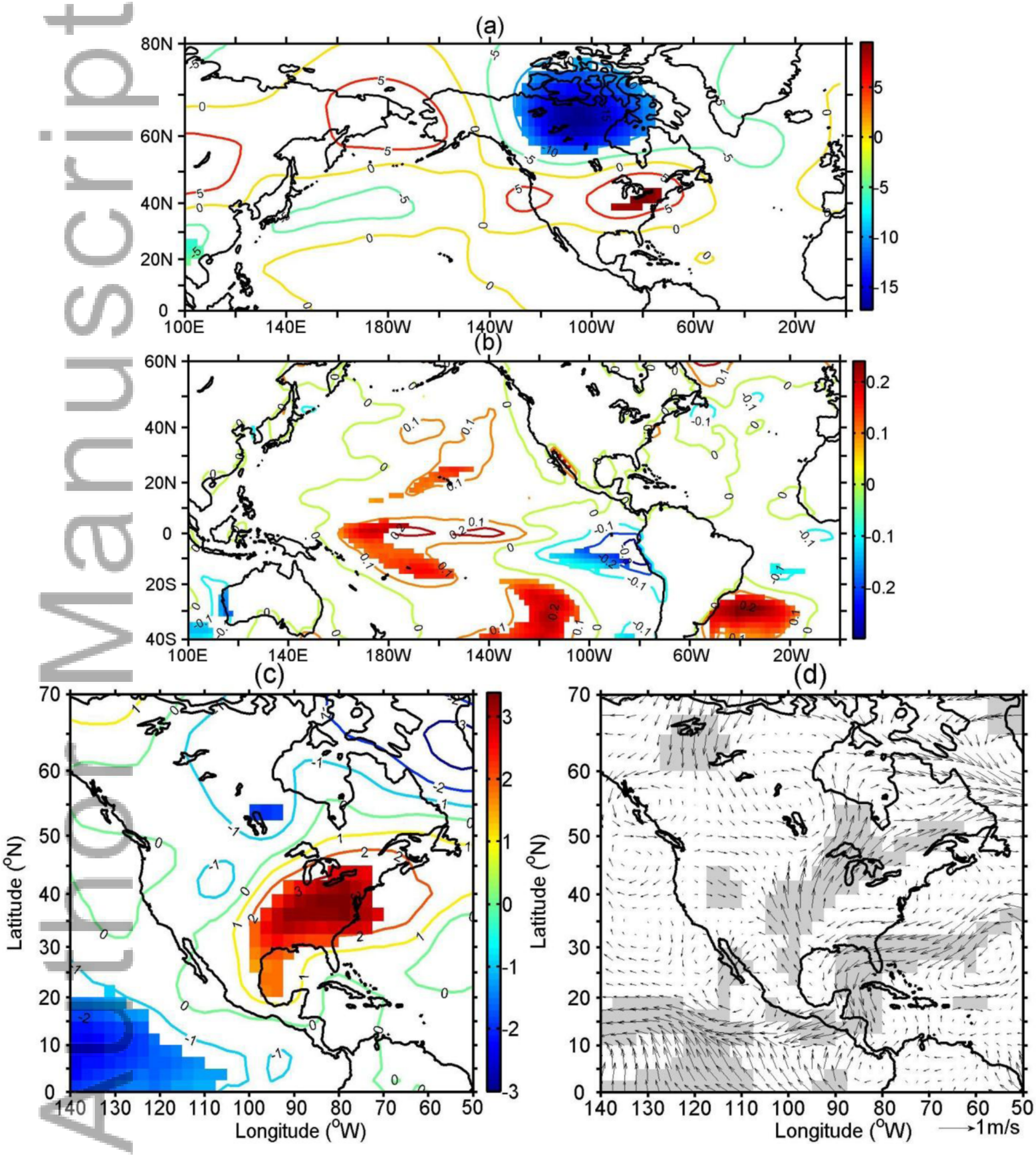
(a)
80N
60N
40N
20N
0
100E
140E
180W
140W
100W
60W
20W
5
0
-5
-10
-15
(b)
60N
40N
20N
0
20S
40S
100E
140E
180W
140W
100W
60W
20W
0.2
0.1
0
-0.1
-0.2
(c)
70
60
50
40
30
20
10
0
140
130
120
110
100
90
80
70
60
50
Latitude (°N)
Longitude (°W)
3
2
1
0
-1
-2
-3
(d)
Latitude (°N)
Longitude (°W)
1m/s

Figure5.tif

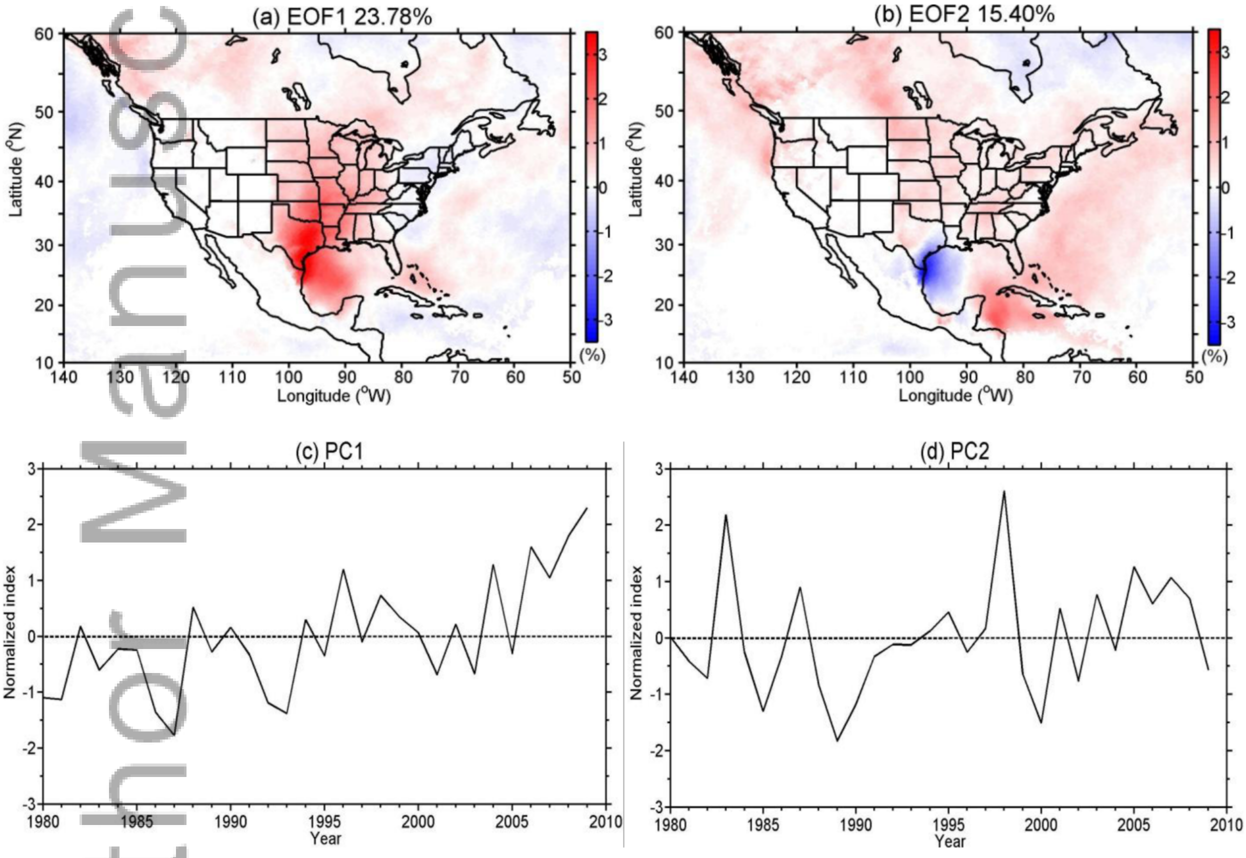
(a) EOF1 23.78%
(b) EOF2 15.40%
Latitude (°N)
Longitude (°W)
60
50
40
30
20
10
140
130
120
110
100
90
80
70
60
50
3
2
1
0
-1
-2
-3
(%)
(c) PC1
(d) PC2
Normalized index
Year
1980
1985
1990
1995
2000
2005
2010

Figure6.tif

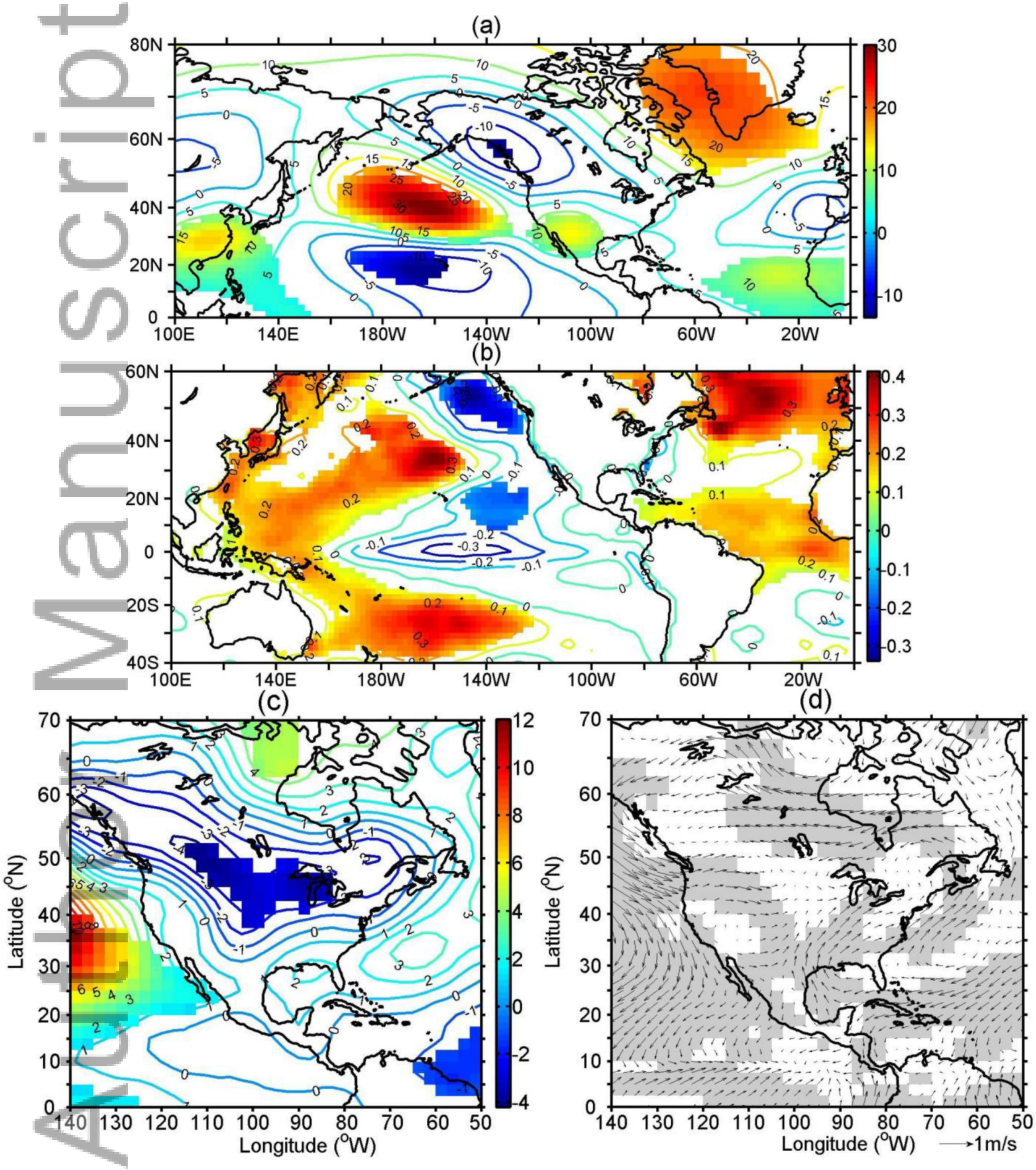
(a)
80N
60N
40N
20N
0
100E
140E
180W
140W
100W
60W
20W
30
20
10
0
-10
(b)
60N
40N
20N
0
20S
40S
0.4
0.3
0.2
0.1
0
-0.1
-0.2
-0.3
(c)
Latitude (°N)
Longitude (°W)
70
60
50
40
30
20
10
0
140
130
120
110
100
90
80
70
60
50
12
10
8
6
4
2
0
-2
-4
(d)
Latitude (°N)
Longitude (°W)
1m/s

Figure7.tif

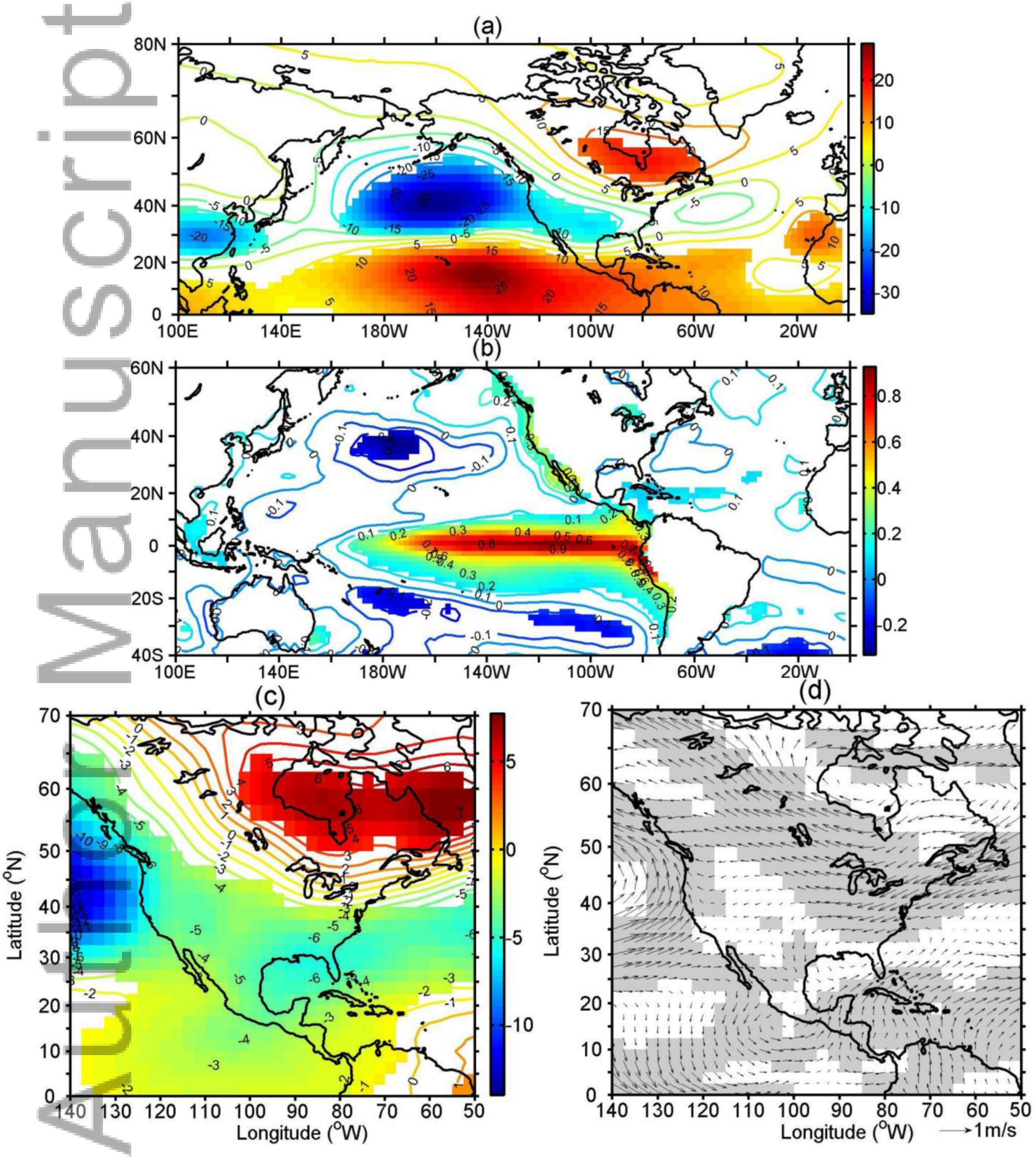
(a)
80N
60N
40N
20N
0
100E
140E
180W
140W
100W
60W
20W
20
10
0
-10
-20
-30
(b)
60N
40N
20N
0
20S
40S
100E
140E
180W
140W
100W
60W
20W
0.8
0.6
0.4
0.2
0
-0.2
(c)
70
60
50
40
30
20
10
0
Latitude (°N)
140
130
120
110
100
90
80
70
60
50
Longitude (°W)
5
0
-5
-10
(d)
70
60
50
40
30
20
10
0
Latitude (°N)
140
130
120
110
100
90
80
70
60
50
Longitude (°W)
1m/s

Figure8.tif